Original Article

Modelling non-ideal detonations in commercial explosives

Paulo José Costa Couceiro Júnior [1]* ⓘ
Juan Navarro Miguel [1]

Abstract

Highly non-ideal explosives usually react expressively below their ideal velocities of detonation. In these cases, dimensional effects and product heterogeneities become important to proper model their respective detonation state. Although Direct Numerical Simulation (DNS) techniques can provide a complete and exact solution for this problem, their actual computation cost are still not practical for industrial applications. In order to minimize these constrains, a simplified two-dimensional steady non-ideal detonation model for cylindrical stick explosives is presented. Based on an ellipsoidal shock shape approach (ESSA), the proposed model combines the quasi-one-dimensional theory for the axial flow solution with the unconfined sonic post-flow conditions at the edge of the explosive. Once calibrated, the model offers the possibility to predict the non-ideal detonation state for any charge diameter, resulting in a full mapping of the diameter-effect curve of the explosive. In addition, the effect of the inert confiner on the detonation flow is calculated by coupling a mechanistic confinement approach with the ESSA model. Thus, the proposed engineering approach is used to model the main properties of one of the most common ammonium nitrate-based explosive used in mining and quarrying industries, including the complete axial flow solution.

Keywords: Non-ideal detonation; Rock blasting; Commercial explosives; Modelling.

Modelagem de detonações não-ideais de explosivos comerciais

Resumo

Explosivos altamente não-ideais tendem a reagir com velocidades de detonação expressivamente inferiores às suas velocidades ideais. Nesses casos, os efeitos dimensionais do problema e heterogeneidades dos produtos se tornam fundamentais para realizar, apropriadamente, a modelagem dos seus respectivos estados de detonação. Ainda que as simulações numéricas diretas (DNS) possam prover uma completa e exata solução para esse problema, seu alto custo computacional ainda é um fator restritivo para sua aplicação prática na indústria. A fim de minimizar estas restrições, um modelo de detonação não-ideal estacionário bidimensional para explosivos cilíndricos é desenvolvido. Baseado na aproximação elipsoidal da frente de choque (ESSA), o modelo proposto se fundamenta na teoria quasi-unidimensional para a solução do fluxo reativo axial, combinando o critério de fluxo sônico após o choque com algumas condições limites na borda da carga explosiva. Uma vez calibrado, o modelo oferece a possibilidade de prever o estado não-ideal de detonação em qualquer diâmetro de carga, resultando no mapeamento completo da curva do efeito-diâmetro do explosivo. Adicionalmente, o efeito do material confinante na detonação é calculado ao acoplar uma aproximação mecanicista do confinamento ao modelo ESSA. Portanto, o modelo proposto é usado para modelar as principais propriedades de um dos explosivos baseados em nitrato de amônio mais comuns na indústria mineira e pedreiras, incluindo a completa descrição do fluxo axial.

Palavras-chave: Detonação no-ideal; Desmonte de rochas; Explosivos comerciais; Modelagem.

[1]Advanced Applied Solutions Department, MAXAM, Madrid, Spain.

*Corresponding author: paulocouceiro@gmail.com

1 Introduction

Ammonium nitrate-based explosives are the most common source of energy used for rock fragmentation and heave. Their nature, composition and heterogeneities, aligned with other characteristics such as multi-dimensional effects and confinement materials, result into a very complex detonation process, with a highly non-ideal behavior. This intrinsically coupled phenomena is still a matter of research and discussion [1-7]. A proper mathematical description of non-ideal detonations requires models where most of these parameters are considered. They must be able to describe the multi-dimensional reactive flow solution of the problem, including pressure profiles, densities and others such as reaction progress and detonation velocities. Several models have been developed for this purpose, such as some classes of direct numerical simulations (DNS) techniques, which are still computationally expensive for a daily-basis application, and a sort of quasi-unidimensional and bidimensional models, like the slightly divergent flow [8] or straight streamline approximation [9].

In this paper, a non-ideal detonation model based on the Ellipsoidal Shock Shape Approach (ESSA) is used to describe the detonation process. The ESSA model is coupled with the Q1D Theory [1] for a proper description of the axisymmetric detonation flow. Once the axial solution is known, the two-dimensional extension is carried out via an ellipsoidal shock shape approach. However, although the explosive-rock interaction could be especially challenged, when combined with a mechanistic model for the confiner material, these models could predict important properties of the resulting detonation structure.

2 Methodology

2.1 Governing equations

The reactive Euler equations for the conservation of mass, momentum and energy (Equation 1)

$$\frac{D\rho}{Dt} + \rho\nabla\cdot\boldsymbol{u} = 0; \rho\frac{D\boldsymbol{u}}{Dt} = -\nabla p; \frac{DE}{Dt} - \frac{p}{\rho^2}\frac{D\rho}{Dt} = 0; \frac{D\lambda}{Dt} = W \quad (1)$$

are often used to describe non-ideal detonations, where $\boldsymbol{u}$ is the velocity; ρ is the density; p is the pressure; E is the internal energy; λ is the reaction progress ($\lambda = 0$, for an unreacted product and $\lambda = 1$ for a complete reaction process); and W is the reaction rate, and the operator $D/Dt = \partial/\partial t + \boldsymbol{u}\cdot\nabla$. The governing equations are closed by defining the equation of state $E(P,\rho,\lambda)$ and the reaction rate $W(P,\rho,\lambda)$.

The governing equations (Equation 1) can be further reduced to describe the axial flow solution of the problem. Although different approaches are available, such as the slightly divergent flow theory [8], the Q1D model [1] is adopted in this study. One of its improvements is the

replacement of the divergent term – which is unknown – by the shock curvature. Since its development, the Q1D model has been demonstrating excellent results regarding the axial flow solutions, even in highly non-ideal detonations [5].

The mathematical foundation of the Q1D theory is discussed elsewhere [1,10,11]. Thus, the resulting set of ordinary differential equations are

$$\frac{du_n}{dn} = \left(\frac{1}{c^2 - u_n^2}\right)\left[Q(\gamma^* - 1)W + \frac{\kappa}{(1 + n\kappa)}c^2(u_n + D_n)\right] \quad (2)$$

$$\frac{d\rho}{dn} = \left(\frac{1}{c^2 - u_n^2}\right)\left[-Q(\gamma^* - 1)\rho\frac{W}{u_n} + \frac{\kappa}{(1 + n\kappa)}\rho u_n(u_n + D_n)\right] \quad (3)$$

$$\frac{d\lambda}{dn} = \frac{W}{u_n} \quad (4)$$

where u_n is the normal particle velocity; ρ is the density; D_n is the normal velocity of detonation; c is the sound speed; Q is the heat of explosion; γ is the adiabatic gamma and W is the reaction rate.

The set of ordinary differential equations form an eigenvalue problem in κ or D_n (Equations 2, 3 and 4). The most common solution strategy is the shooting method subjected to the jump shock and generalized CJ conditions [1,12,13]. In this paper, the following quadratic pseudo-polytropic equation of state is used

$$E = \frac{P}{(\gamma^* - 1)\rho} - \lambda Q \quad \gamma^* = \gamma_o + \gamma_1\frac{\rho}{\rho_o} + \gamma_2\left(\frac{\rho}{\rho_o}\right)^2 \quad (5)$$

where ρ is the density; ρ_o is the initial density Q is the heat of reaction; γ^* is the quadratic gamma; γ_o, γ_1 and γ_2 are coefficients obtained from an ideal thermodynamic detonation code. On the other hand, the reaction rate equation is given by a simple pressure-dependent equation

$$W = \frac{1}{\tau}(1 - \lambda)^m\left(\frac{P}{P_{ref}}\right)^n \quad (6)$$

where n, m and τ are reaction rate parameters and P_{ref} is a reference pressure. Assuming a strong shock approximation, the pressure P can be expressed as

$$P = \frac{(\gamma^* - 1)\rho}{\gamma^*}\left[\frac{D_n^2 - u_n^2}{2} + Q\lambda\right] \quad (7)$$

2.2 Two-dimensional expansion: an ellipsoidal shock shape approach

Experimental shock front measurements – supported by Direct Numerical Simulations – show evidence that it can be well represented by the following arc of ellipse [1,14]

$$\frac{(z_f + \alpha)^2}{\alpha^2} + \frac{r^2}{\beta^2} = 1 \quad (8)$$

where z and r are the axial and radial directions, respectively; and α e β are the ellipse semi-axis, called in this study as the shock shape parameters.

In the ESSA model, the axial flow solution is intimately associated with the shape of the detonation shock front. This relationship is addressed by relating the axisymmetric curvature κ with the shock shape parameters α and β via the second derivative of the shock front function z_f, which express the curvature at any point along of the shock. Thus, for a given velocity of detonation D_n and reaction rate parameters , m and τ, z_f'' can be related to the axisymmetric cylinder shock front curvature κ_{axis}, at $r = 0$, by

$$\beta = \left(\frac{2\alpha}{\kappa_{axis}} \right)^{1/2} \tag{9}$$

where α e β are the shock shape parameters.

Equation 9 is essential to ensure a proper dependence between shock shape parameters and the axial solution. The next step is the definition of boundary conditions at the explosive's edge. The first condition is defined in terms of the shock slope, where the post-shock flow must be exactly sonic [15], which means that the first derivative of Equation 8 must be sonic at the unconfined charge edge, $r = R$.

Nevertheless, the ellipsoidal shock shape hypothesis presents several possible sonic solutions at different charge radius. Therefore, an additional boundary condition must be defined at the explosive edge. This second condition is addressed by assuming that the charge radius R is smaller than the semi-major axis of the ellipse z_f, so that $R_{max} = \beta$. Hence, the ratio between the charge radius and the semi-major axis can be established as $f_n = R / R_{max}$, where f_n is an expression which relates the degree of non-ideality of the explosive. Thus, f_n is defined as a dimensionless expression such as

$$f_n = 1 - f_a \left[(1 - \lambda)^m \frac{D_o}{D_{CJ}} \right]^{1/2} \tag{10}$$

where λ is the axial reaction progress at the sonic locus; m is a reaction rate parameter; D_o is the velocity of detonation; and D_{CJ} is the thermodynamic ideal velocity of detonation; f_a is a function dependent of the pressure and adiabatic coefficient.

Therefore, the calculation consists in determining the unconfined charge radius R – for a given unconfined velocity of detonation and reaction rate parameters – by relating the axial flow solution, shock shape parameters and the sonic boundary condition at the charge edge.

2.3 Confinement model

In this paper, the confinement effect is structured according to the ideas proposed by Eyring et al. [16] and Souers et al. [17]. A simple inspection of unconfined and confined diameter-effect curves shows evidence of how the confinement tends to increase the detonation velocity for a given diameter. Hence, for a given velocity of detonation, the confinement effect allows its propagation in an even smaller explosive diameter. Thus, a ratio between the unconfined R_u and confined R_c charge radius can be defined as

$$\frac{R_u}{R_c} = f_c \tag{11}$$

where f_c is the confinement factor. This ratio must be proportional to the properties of the explosive, confiner material and its thickness. Here, the confinement is described by

$$f_c = \left[1 + \frac{1}{f_z} \frac{\rho_c C_c}{\rho_o D_o} \right]^{\frac{C_c}{D_o}} \tag{12}$$

where ρ_c and C_c are the density and the seismic velocity of the confiner, respectively; ρ_o and D_o are the explosive density and the velocity of detonation, respectively; f_z is the artificial pre-compression factor due to the subsonic coupling ($f_z = 1$ for supersonic; and $f_z > 1$ for subsonic).

3 Essa model validation

A simple polytropic equation of state with $\gamma = 3$ is examined for non-dimensional unconfined detonations. Calculations were performed for $m = 0.5$ and various n (see Equation 6) and compared with Watt et al. [9] results. As can be seen in Figure 1a and b, diameter curve predictions for $n = 0$ and $n = 1$ are in very good agreement with DNS calculation. This is a good sign since the severest non-ideal detonation cases are very low state dependent [9].

In comparison with SSA model, the ESSA model seems to improve the overall diameter effect curve for larger radii, whereas it is almost equivalent for smaller diameters for $n = 0$ and slightly higher for $n = 1$.

Moving to higher values of n, ESSA model has presented notable improvements over Q1D DSD and SSA models, especially for $n = 1.7$, as can be seem in Figure 1c. Very good predictions could be achieved for all large and small radii. In this case, the critical diameter predicted by the ESSA is slighter smaller than the predicted by the SSA model [9], although the DNS curve seems to predict even smaller critical diameter.

Nevertheless, for $n = 2$, shown in Figure 1d, the ESSA model well predicts medium-larger radii while over-estimates the critical diameter when compared to the DNS [9]. In this case, the SSA model better predicts the critical diameter in comparison with the ESSA. However, the most interesting diameter sizes are the medium-larger ones because of its practical application in mining and blasting operations. Surprisingly, the ESSA model has achieved interesting results predictions for medium-larger diameters, not only for $n = 2$, but in all other scenarios.
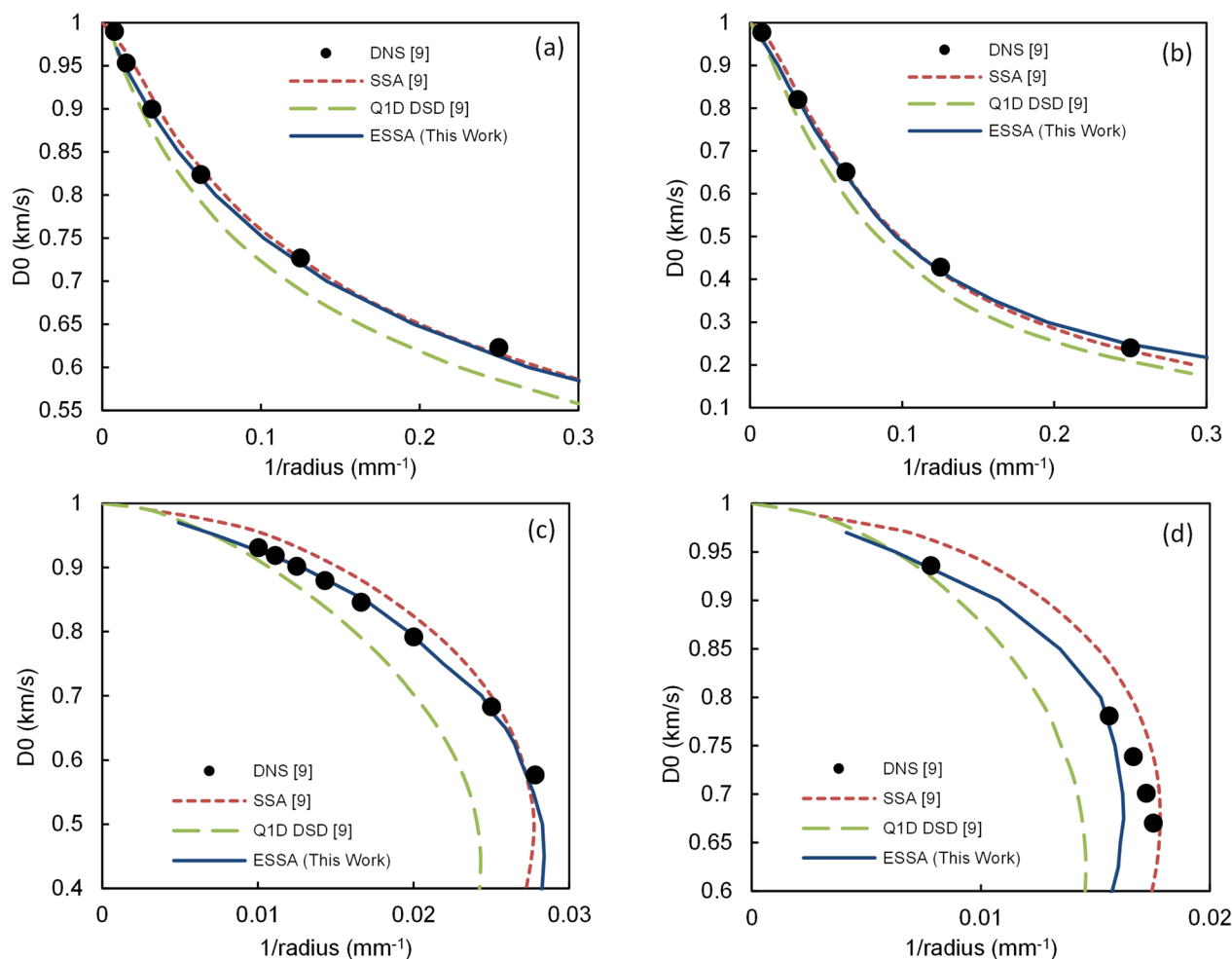
Figure 1. Diameter effect curve for cylindrical-stick geometry. Solid line (ESSA), dotted lines (SSA [9]), dashed lines (Q1D DSD [9]) and circles (DNS [9]).

Table 1. Ideal thermodynamic data

Explosive	D_{CJ}	ρ_0	Q	γ_0	γ_1	γ_2
ANFO	4800 m/s	800 kg/m³	3822 kJ/kg	1.3333	0.36264	0.076288

4 Results and discussions

The potential application of the ESSA model in reliable rock blasting simulations is assessed by modelling the influence of limestone confinement on the ANFO's detonation state in several blasthole diameters. The experimental unconfined diameter-effect curve, necessary to proper calibrate the reaction rate parameters, is obtained from Kirby et al. [18].

The thermodynamic characterization, which includes its ideal velocity of detonation, heat of explosion and the quadratic coefficients of the isentropic gamma (Table 1), were taken from Sharpe and Braithwaite [1].

The ESSA model presents an attractive reaction rate fitting capabilities due to its low computational cost. Since it is coupled with the Q1D model [1], the specific set of reaction rate parameters, responsible to match the predicted

diameter-effect curve to the experimental data, can be found by non-linear minimization techniques. Thus, applying this fitting strategy to the unconfined ANFO data [18], the values of n, m and τ were obtained and presented in Table 2. Note that a pressure exponent of $n = 1.78$ was required to reproduce the experimental diameter-effect curve. There is always a presence of an inflexion point in diameter-effect curves when $n \geq 1.5$ [19], which is associated with the failure diameter of the explosive [9,15]. The modelled unconfined diameter-effect curve predicts a failure diameter very close to the experimental data. See the complete unconfined curve in Figure 2.

On the other hand, the reproduction of real-scale confined detonation experiments in laboratories are restrictive due to the charge sizes. Consequently, the validation of non-ideal detonation models usually tends to be carried out

against real production blasthole measurements, normally through the in-hole confined velocity of detonation. In real applications, the velocity of detonation can be a good indicator of the degree of non-ideality of a given explosive [20]. In this study, a set of in-hole detonation velocities were taken from real-scale field measurements, specifically for a confined ANFO detonation in limestone. The experimental and calculated results are shown in Table 3. The mechanical properties of the limestone are 2450 kg/m^3 and 4120 m/s, as density and seismic velocity, respectively.

Table 2. Reaction rate parameters

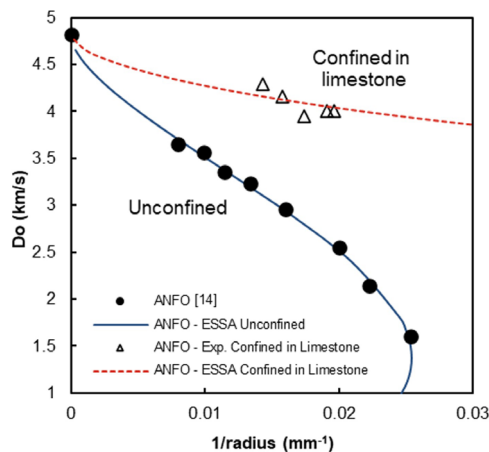| Explosive	m	n	τ
ANFO	2.19	1.78	2.82(-05)

Figure 2. Predicted and experimental unconfined and confined velocity of detonation in limestone.

Once the unconfined non-ideal detonation structure is modelled for a given velocity of detonation (or diameter), the equivalent confined non-ideal detonation state can be calculated. The confined diameter-effect curve in limestone is obtained by imposing the confinement factor (Equations 11 and 12) over the unconfined curve. The modelled confined velocities of detonation and their comparison with the experimental measurements is presented in Table 3 and Figure 2. In general, the overall results were good, especially when considering the experimental scatter of the data, presenting relative errors less than 3.7%.

In non-ideal explosives, the detonation shock front is curved due to the lateral expansion exerted by the confining material. In this case, the detonation driving zone – the region formed between the shock and sonic locus – presents a clear interface with the rock material. This interface is the place where the explosive-rock couple process takes place, being the rock response a function of the explosive loading along the blasthole wall [21]. The energy generated within the DDZ is responsible of auto-supporting the detonation wave. Thus, in order to better understand this process, predictions of the ANFO detonation structure in a blasthole diameter of 127 mm were carried out for both unconfined and confined (in limestone) cases.

Figure 3a and 3b show the non-ideal unconfined and confined detonation structures of an ANFO in a charge diameter of 127 mm. Strong differences on the overall DDZ structures are evident, which can be further realized through the detonation properties at the sonic locus (equivalent of the Chapman-Jouguet state), shown in Figure 4. Firstly, as expected, a much more curved detonation shock front - and larger deflexion angles – are observed in the unconfined

Table 3. Experimental and modelled confined ANFO velocities of detonation in limestone

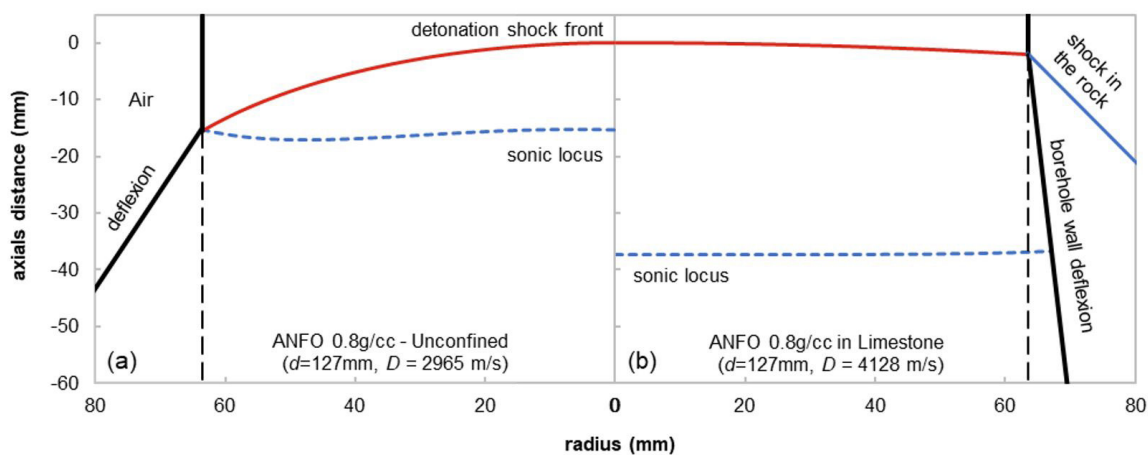| d	102 mm	105 mm	115 mm	127 mm	140 mm
D_{o_ex}	4006 ± 21 m/s	4009 ±104 m/s	3946 m/s	4162 ± 86 m/s	4290 ± 6 m/s
D_{o_cal}	4045 m/s	4056 m/s	4091 m/s	4128 m/s	4163 m/s
Relative error	1.0%	1.2%	3.7%	-0.8%	-3.0%

Figure 3. Predictions of the (a) unconfined and (b) confined (in limestone) ANFO detonations structure in a blasthole diameter of 127 mm. Unconfined D=2965 m/s and confined D=4128 m/s.
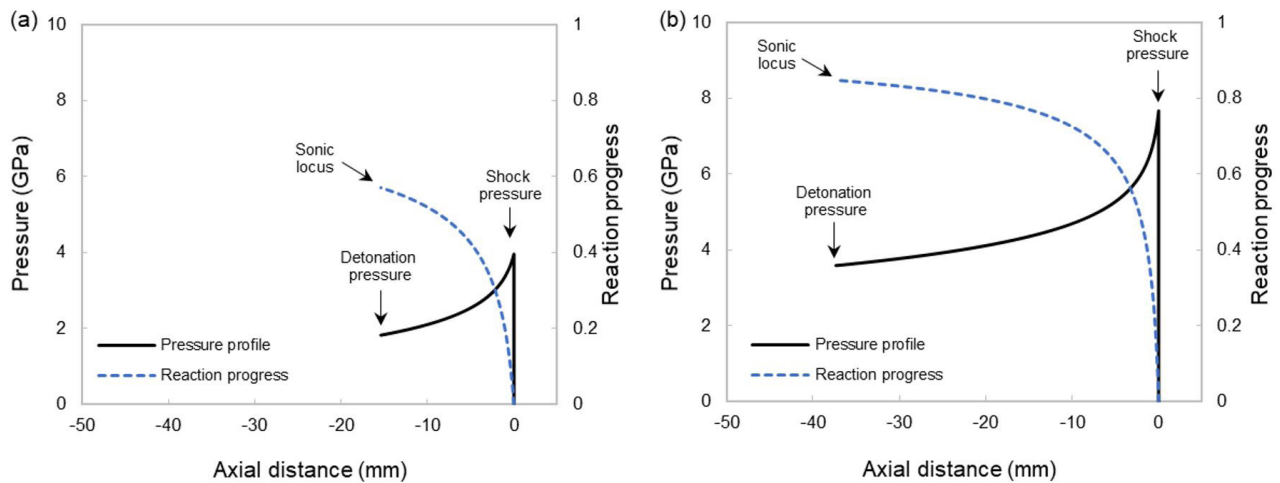
Figure 4. Prediction of the axial pressure and reaction progress profiles in a blasthole diameter of 127 mm, for (a) unconfined and (b) confined (in limestone) ANFO detonations. Unconfined D=2965 m/s and confined D=4128 m/s.

Table 4. Confined detonation results (ANFO)

d	Type	D	P	λ	n
127 mm	Unconfined	2965 m/s	1.82 GPa	0.570	-15.4 mm
127 mm	Confined	4128 m/s	3.58 GPa	0.847	-37.4 mm

detonation case. Another aspect to note is the length of the effective reaction zone, which is more than 2 times bigger in the case of the confined detonation. Additionally, the confinement imposed by the limestone favored to a higher chemical release process within the detonation driving zone, supporting the propagation of a higher velocity of detonation, around 39% higher than the unconfined case.

The confinement effect contributes to burn around 84.7% of the explosive within the axial reaction zone while only 57% is reacted in the case of unconfined detonation (Table 4). Indeed, for a given charge diameter, the ANFO burns more rapidly in the confined detonation cases than in the unconfined ones. This burning release process can be further observed on the axial pressure and reaction progress profiles presented in the Figure 4.

5 Conclusions

The Ellipsoidal Shock Shape Approach (ESSA) for modelling two-dimensional steady non-ideal detonation was presented. The proposed model can describe the complete unconfined diameter-effect curve of the explosive once the reaction rate parameters are fitted to a set of experimental data. The results obtained for the ANFO were excellent, including the prediction of its failure diameter. When coupled with the confinement properties, the ESSA model can readily represent the expected confined detonation state of the explosive. Experimental in-hole detonation velocities were used to check the model response to the confined detonation cases. The results showed a good agreement to the different blasthole diameters, even considering the scatter of the experimental data. Both confined and unconfined detonation structures, alongside their correspondent axial pressure and reaction progress profiles, were studied in order to better understand the macro-interaction between the explosive and the rock material. Thus, the overall performance, aligned with its simplicity, suggests the ESSA model as a reliable source of explosive's energy information for a more realistic rock blasting simulation.

References

1 Sharpe GJ, Braithwaite M. Steady non-ideal detonations in cylindrical sticks of explosives. Journal of Engineering Mathematics. 2005;53:29-58.
2 Sharpe GJ, Bdzil JB. Interactions of inert confiners with explosives. Journal of Engineering Mathematics. 2006;54:273-298.

3   Sellers EJ. Velocity of detonation of non-ideal explosives: investigating the influence of confinement. In: International Society of Explosives Engineers. Proceeding of the 33rd Annual Conference on Explosives and Blasting Technique; 2007 January 28-31; Nashville, Tennessee, USA. Nashville: ISEE; 2007. Vol. 2, p. 1-11.

4   Esen S. A non-ideal detonation model for evaluating the performance of explosives in rock blasting. Rock Mechanics and Rock Engineering. 2008;41(3):467-497.

5   Sharpe GJ, Luheshi MY, Braithwaite M, Falle S AEG. Steady non-ideal detonation. Shock Compression of Condensed Matter. 2009;1195:452-457.

6   Sellers E, Furtney J, Onederra I, Chitombo G. Improved understanding of explosive–rock interactions using the hybrid stress blasting Model. Journal of the Southern African Institute of Mining and Metallurgy. 2012;112(8):721-728.

7   Braithwaite M, Sharpe GJ. Non-Ideal detonation behavior in commercial explosives. In: Fragblast. Proceeding of the 10th Symposium on Rock Fragmentation by Blasting. Performance of Explosives and New Developments; 2012 November 26-29; New Delhi, India. New Delhi: FRABLAST; 2013. p. 11-16.

8   Kirby IJ, Leiper GA. A small divergent detonation theory for intermolecular explosives. In: Office of Naval Research. Proceeding of the 8th Symposium (International) on Detonation. NSWC MP 86-194. 1985 July 15-19; Albuquerque, NM, USA. Albuquerque: Naval Surface Weapons Center; 1985. p. 176-186.

9   Watt SD, Sharpe GJ, Falle SA, Braithwaite M. A streamline approach to two-dimensional steady non-ideal detonation: the straight streamline approximation. Journal of Engineering Mathematics. 2012;75(1):1-14.

10   Stewart S. Lectures on detonation physics: Introduction to the Theory of Detonation Shock Dynamics. WL-TR-94-7089. Champaign: University of Illinois; 1993.

11   Yao J, Stewart DS. On the dynamics of multi-dimensional detonation. Journal of Fluid Mechanics. 1996;309:225-275.

12   Stewart DS, Yao J. The normal detonation shock velocity-curvature relationship for materials with nonideal equation of state and multiple turning points. Combustion and Flame. 1998;113:224-235.

13   Sharpe G. The structure of planar and curved detonation waves with reversible reactions. Physics of Fluids. 2000;12(11):3007-3020.

14   Kennedy DL. Multi-valued normal shock velocity versus curvature relationships for highly non-ideal explosives. In: Office of Naval Research. Proceeding of the 11th Symposium (International) on Detonation. 1998 August 30 - September 4; Snowmass, Colorado, USA. Arlington: Office of Naval Research; 1998. p. 181-192.

15   Cartwright M. Modelling of non-ideal steady detonations [PhD thesis]. Leeds: University of Leeds; 2016.

16   Eyring H, Powell RE, Duffey GH, Parlin RB. The stability of detonation. Chemical Reviews. 1949;45(1):69-181.

17   Souers PC, Vitello P, Esen S, Bilgin HA. The effects of containment on detonation velocity. Propellants, Explosives, Pyrotechnics. 2004;29(1):19-26.

18   Kirby I, Chan J, Minchinton A. Advances in predicting the effects of non-ideal detonation on blasting. In: International Society of Explosives Engineers. Proceeding of 40th Annual Conference on Explosives and Blasting Technique; 2014 February 9-12; Denver, Colorado, USA. Denver: ISEE; 2014. p. 1-14.

19   Cowperthwaite M. An exact solution for axial-flow in cylindrically symmetrical, steady state detonation in polytropic explosive with an arbitrary rate of decomposition. Physics of Fluids. 1994;6(3):1357-1378.

20   Bilgin HA, Esen S. Assessment of ideality of some commercial explosives. In: International Society of Explosives Engineers. Proceedings of the 25th Annual Conference on Explosives & Blasting Technique; 1999 February 7-10; Nashville, Tennessee, USA. Nashville: ISEE; 1999. p. 35-44.

21   Sharpe GJ, Braithwaite M. Blast modelling towards a predictive model for the performance of commercial explosives in rock blasting. Quarry Management. 2013;2:22-28.